

1 **Luminescent Metallo-BODIPYs****Chiral-at-Metal BODIPY-Based Iridium(III) Complexes: Synthesis and Luminescence Properties**Marta G. Avello,<sup>[a,d]</sup> María C. de la Torre,<sup>\*,[a,d]</sup> Andrés Guerrero-Martínez,<sup>[b]</sup>  
Miguel A. Sierra,<sup>\*,[c,d]</sup> Heinz Gornitzka,<sup>[e]</sup> and Catherine Hemmert<sup>[e]</sup>

**Abstract:** The synthesis of enantiomerically pure Ir(III) complexes with one or two BODIPY moieties has been achieved through the enantioselective C–H insertion from homochiral triazolium salts, containing a sulfoxide functionality in their structures. These homochiral salts were prepared by the sequential Cu-catalyzed alkyne-azide cycloaddition (CuAAC) of an azide and one alkynyl sulfoxide, followed by a Suzuki coupling in the preformed triazol with a BODIPY containing aryl boronic acid, followed by methylation of the N3-triazole nitrogen. The configuration at the metal in these chiral complexes was established

by using a combination of CD and X-ray diffraction techniques. The optical properties of these complexes were thoroughly studied using spectroscopic (absorption and fluorescence) and computational (TD-DFT and DFT) methods. The fluorescence of complexes with the BODIPY attached to the sulfoxide moiety (including the two BODIPYs-based complex) was quenched upon introduction of the Ir(III) fragment, most likely due to an  $\alpha$ -PET mechanism. On the contrary, the fluorescence of Ir(III) complexes with the BODIPY attached to the triazolium ring remains unquenched.

26 **Introduction**

Interest in transition metal complexes having the chromophore 4,4-difluoro-4-bora-3a,4a-diaza-*s*-indacene (BODIPY) systems<sup>[1]</sup> has increased during the last years. The large number of available structural modifications, due to the presence of the metal compared to the full organic counterparts, allows modulation of the optoelectronic properties of the complexes, as well as their use in different fields ranging from biological labelling to dynamic phototherapy.<sup>[2]</sup> In return, deactivation of the fluorescence by the presence of the metal is frequently observed.

Nevertheless, different and relevant photophysical properties may emerge depending on the mechanism of photodeactivation.<sup>[3]</sup>

The incorporation of a transition metal center to the BODIPY can be done either by bonding the metal to the peripheries of the BODIPY or directly to the  $\pi$ -conjugated system of this fluorophore. In this regard, the incorporation of a transition metal to a BODIPY through a *N*-heterocyclic carbene ligand (NHC) has been reported. Thus, Plenio described the synthesis of several BODIPY-NHC complexes, including Ru(III), Ir(III), Rh(III), Ir(I), Rh(I), Pd(II) and Au(I) complexes.<sup>[4]</sup> Additionally, the preparation of Hoveyda-Grubbs catalysts having a BODIPY moiety coordinated to the Ru(I) through the NHC moiety has been reported and used to follow the metathesis mechanism through fluorescence correlation spectroscopy.<sup>[5]</sup> Similarly, Ir(I) complexes have been prepared<sup>[6]</sup> and used for hydrogen detection. Recently, Albrecht has reported the preparation of the first Pd(II) and Ir(II)-1,2,3-triazolylidene complexes and their use in monitoring displacement of ligand reactions.<sup>[7]</sup> In these cases, the changes in the intensity of the emission of the resulting complexes was an adequate probe to study these processes.

During our work in the synthesis of transition metal complexes having 1,2,3-triazolylidene (MIC) ligands with enantiopure sulfoxide and sulfoximine moieties,<sup>[8]</sup> we have reported the role of the chiral mesoionic carbene ligand (MIC) in defining the catalytic reactivity of their Au(I) derivatives,<sup>[9]</sup> preparing enantiopure chiral at metal complexes,<sup>[10]</sup> and enantiopure complexes having chiral-at-metal and chiral planar metallocene moieties.<sup>[11]</sup> On the other hand our work in push-pull systems containing a Cr(0) and W(0) Fischer metal carbene moiety, I, clearly demonstrated that the system geometry is reflected in the deactivation of the fluorescence.<sup>[12]</sup> Analogously, complexes

[a] Dr. M. G. Avello, Dr. M. C. de la Torre  
Instituto de Química Orgánica General, Consejo Superior de Investigaciones Científicas (IQOG-CSIC),  
Juan de la Cierva 3, 28006 Madrid, Spain  
E-mail: mc.delatorre@csic.es  
www.iqog.csic.es/es/directory/maria-del-carmen-de-la-torre-egido

[b] Prof. A. Guerrero-Martínez  
Departamento de Química Física, Facultad de Química Universidad Complutense,  
28040 Madrid, Spain

[c] Prof. M. A. Sierra  
Departamento de Química Orgánica I, Facultad de Química Universidad Complutense,  
28040 Madrid, Spain  
E-mail: sierraor@ucm.es  
www.biorganomet.es

[d] Dr. M. G. Avello, Dr. M. C. de la Torre, Prof. M. A. Sierra  
Centro de Investigación en Química Avanzada (ORFEO-CINQA),  
Universidad Complutense,  
28040 Madrid, Spain

[e] Prof. H. Gornitzka, Prof. C. Hemmert  
LCC-CNRS, Université de Toulouse, CNRS, UPS,  
Toulouse, France

Supporting information and ORCID(s) from the author(s) for this article are available on the WWW under <https://doi.org/10.1002/ejic.202000745>.

BODIPY-metal carbene **II**, having remote  $\pi$ -conjugation, allowed to determine the influence of electronic factors in the emission properties of the BODIPY moiety.<sup>[13]</sup> A similar study was carried out in BODIPYs having remote half-sandwich Ir(III) and Rh(III) moieties, **III** (Figure 1).<sup>[14]</sup>

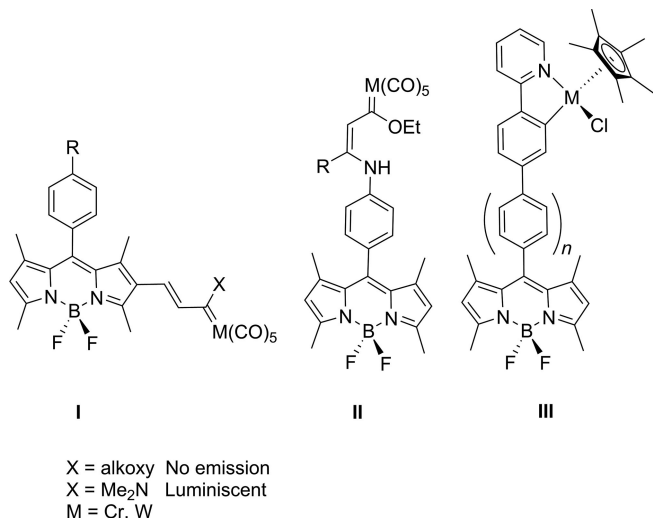
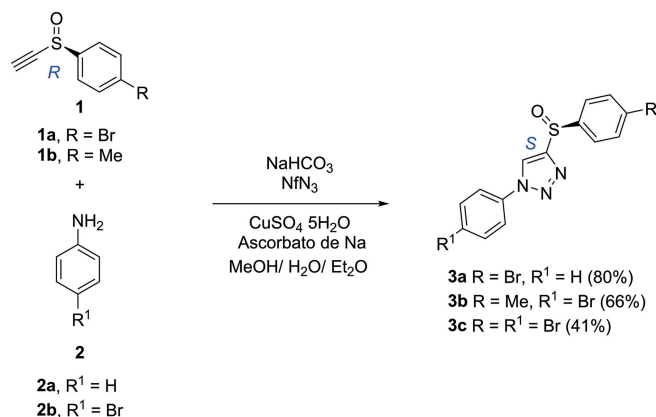


Figure 1. Previously studied Fischer metal carbene BODIPYs push-pull systems (**I**, **II**) and BODIPYs having remote half-sandwich Ir(III) and Rh(III) (**III**).

Circularly polarized emission (CPL) is rarely observed in systems different from chiral organic molecules<sup>[15]</sup> and lanthanide complexes.<sup>[16]</sup> To the best of our knowledge, studies searching for CPL in chiral-at-metal BODIPY containing molecules has not been reported. Our previous work in the field opens an opportunity to watch the possibility of observing CPL in this class of molecules. We now report on the synthesis of homochiral half-sandwich Ir(III) complexes having one or two BODIPY moieties coordinated to the metal by a sulfoxide containing MIC ligand, as well as the study of their chiroptical and photophysical properties. To the best of our knowledge, this is the first time that homochiral transition metal-MIC BODIPYs have been reported.

## Results and Discussion

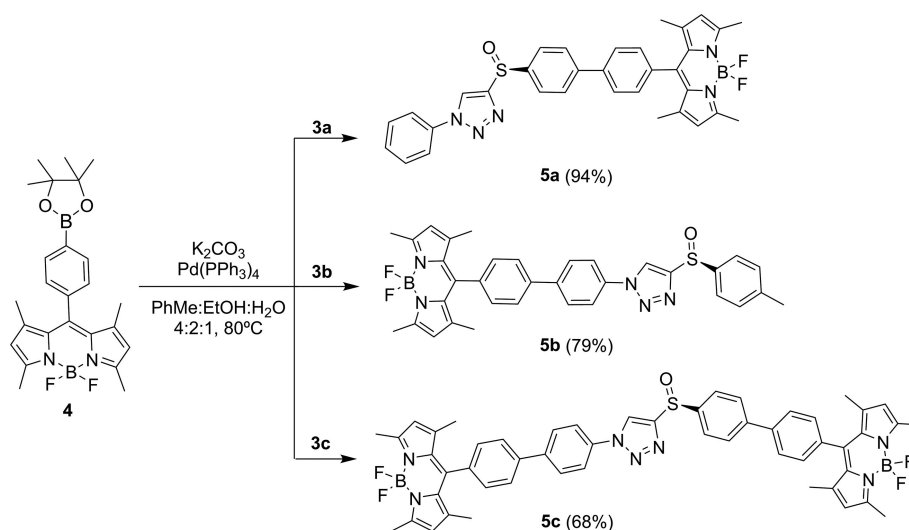
Access to the three different structural types of 1,2,3-triazole- BODIPY derivatives considered in this study was gained by using enantiopure alkynyl sulfoxides **1** and anilines **2**. Three differently substituted 1,2,3-triazolyl sulfoxides **3** were obtained by reaction of NfN<sub>3</sub> (nonafluorobutanesulfonyl or nonafllyl azide) and the corresponding aniline to generate “in situ” the azide,<sup>[17]</sup> and subsequent Cu-catalyzed azide-alkyne cycloaddition in mixtures MeOH/H<sub>2</sub>O/Et<sub>2</sub>O as solvent, using CuSO<sub>4</sub>·5H<sub>2</sub>O/sodium ascorbate as the catalyst.<sup>[8]</sup> The yields on compounds **3** were acceptable to good (41–80 %) (Scheme 1).



NfN<sub>3</sub> = nonafluorobutanesulfonyl azide

Scheme 1. Synthesis of triazoles **3** by CuAAC between “in situ” generated azides and enantiopure alkynes **1**.

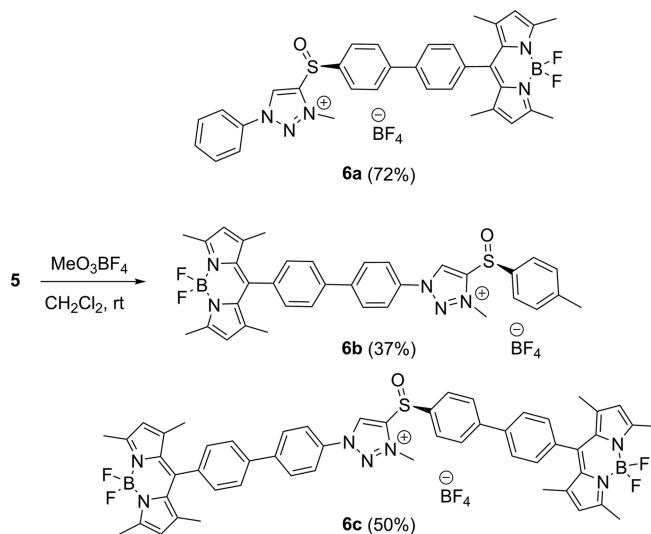
Pinacolyl derivative **4** was prepared following literature procedures<sup>[18]</sup> and coupled with triazolyl sulfoxide **3a** using Pd(PPh<sub>3</sub>)<sub>4</sub>/K<sub>2</sub>CO<sub>3</sub> in a mixture toluene/EtOH/H<sub>2</sub>O (4:2:1) as the coupling conditions. Thus, these conditions, which formed the triazolyl-BODIPY **5a** in 94 % yield, were used in the preparation of the two additional structural types studied in this work. Thus, coupling of sulfoxide **3b** with BODIPY **4** formed compound **5b** in 79 % yield. Compound **5c** having two BODIPY subunits was



Scheme 2. Suzuki coupling to prepare BODIPY derivatives **5**.

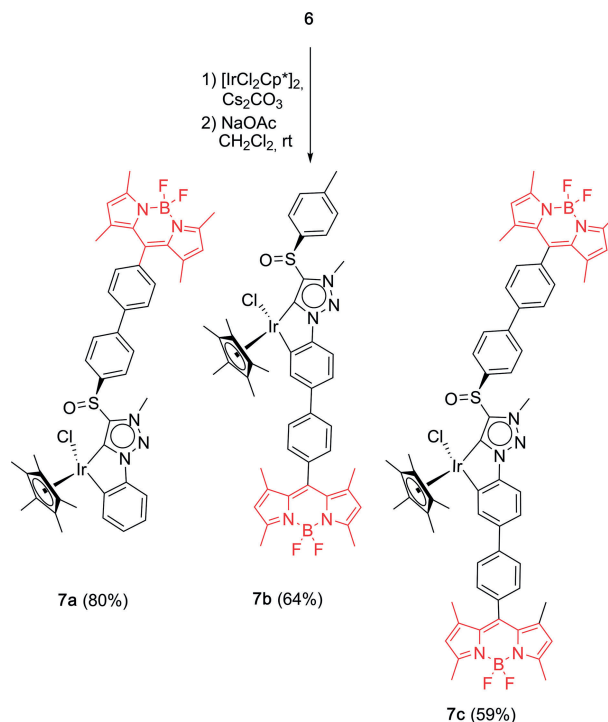
obtained from 1,2,3-triazole **3c** through a double Suzuki coupling in a 68 % yield (Scheme 2). Spectroscopic and spectro-  
106 metric data confirm the structures of compounds **3–5**. Compounds **5** were highly colored (orange-green), luminescent products.

Compounds **5** were methylated with  $\text{Me}_3\text{OBF}_4$  using the standard conditions to yield the corresponding triazolium salts **6** in acceptable to good yields (37 % to 72 %) (Scheme 3). Triazolium salts **6** (also strongly colored and fluorescent products) were treated with  $[\text{IrCl}_2\text{Cp}^*]_2$  in the presence of  $\text{Cs}_2\text{CO}_3$ . In these conditions a mixture of two products, identified as the desired cyclometallated Ir complexes **7** and their  
116 non-cyclometallated dichloro Ir-precursors, was obtained. The exclusive formation of cyclometallated Ir complexes **7**, was effected by the sequential treatment of salts **6** with  $[\text{IrCl}_2\text{Cp}^*]_2$  and  $\text{Cs}_2\text{CO}_3$  until disappearance of the signal corresponding to the H5 of the triazolium ring (8.89–8.94 ppm), followed by treat-  
121 ment of the reaction mixtures with NaOAc, in a one-pot manipulation. In these conditions iridacycles **7a** and **7b** were obtained in 80 % and 64 % yields, respectively, and bis-iridacycle **7c** in 59 % yield (Scheme 4). Compounds **7** having one new chiral-  
126 at-metal stereocenter were obtained as single enantiomers. Tra- ces of the corresponding diastereomers (enantiomers at the metallic chiral centers) were not observed in the  $^1\text{H}$  NMR spectra of the reaction crude materials.



Scheme 3. Methylation of triazoles **5** to obtain the corresponding triazolium salts **6**.

The structure of compounds **7** was determined on spectroscopic grounds. Thus,  $^{13}\text{C}$  NMR spectra of complexes **7** show  
131 two new quaternary carbon signals assignable to the carbene carbon (156.2 and 156.3 ppm for **7a** and **7b–c**, respectively), and to the metallated aromatic carbon (144.0 and 145.2 ppm for **7a** and **7b–c**, respectively), which is in accordance with the metallation and the C–H activation reactions. The most charac-  
136 teristic feature of the  $^1\text{H}$  NMR spectra of iridacycles **7** was the disappearance of the signal corresponding to the H5 of the 1,2,3-triazole ring in the salts **6** (8.89–8.94 ppm), confirming the coordination of the MIC ligand. Finally, a single crystal of complex **7b** was obtained by slow diffusion in a  $\text{CH}_2\text{Cl}_2$ /pentane



Scheme 4. The synthesis of enantiopure Ir complexes **7** having BODIPY moieties.

mixture. The structure and the absolute stereochemistry of 141 complex **7b** was then unambiguously established by X-ray diffrac- tion (Figure 2).

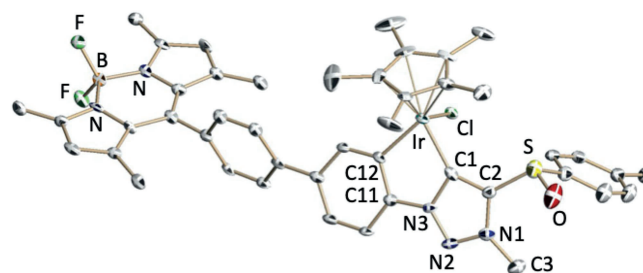


Figure 2. X-ray structure of complex **7b** depicted at a 30 % thermal ellipsoid level. Selected bond lengths [Å] and angles [°]: Ir–C1 2.00(2), Ir–C12 2.06(2), Ir–Cl 2.39(1), C1–C2 1.39(2), C2–N1 1.39(2), N1–N2 1.32(2), N2–N3 1.32(2), C1–N3 1.41(2), C2–S 1.75(2), S–O 1.48(2), N1–C3 1.44(2), N3–C11 1.41(2), C1–Ir–Cl 87.3(3), C1–Ir–C12 79.4(4), C12–Ir–Cl 85.4(3).

Complexes **7** were configurationally stable as established by recording the  $^1\text{H}$  NMR spectra of a solution of these complexes after one week in solution. The absolute configuration of com-  
146 plexes **7** was determined by a combination of circular dichroism and X-ray diffraction as previously established by us for similar piano-stool MIC.<sup>[10]</sup> Figure 3 compiles the CD spectra of compounds **5a**, **6a** and **7a** as representative examples of the compounds studied in this work (see the SI for the comparative CD 151 spectra of the remaining compounds). Triazole **5a** and triazolium salt **6a** are less absorptive than the iridium complex **7a**. Thus, compounds **5** and **6** always show positive dichroic signals centered at 261.0–285.8 nm and 282.4–292.4 nm respec-  
156 tively, while Ir(III) complexes have a strong negative Cotton ab-

sorption in the range of 253.8 to 290.4 nm. This strong negative Cotton absorption is maintained (287.0 nm) for the Ir(III) complex **7c**.<sup>[19]</sup> In previous studies,<sup>[10]</sup> this negative Cotton absorption was assigned to an absolute configuration *R* at the metallic center. Since absolute configuration *R* at the Ir(III) for **7b** has been unambiguously established by X-ray analysis (absolute structure factor  $x = 0.013(7)$ ), we can conclude that the absolute configuration at the metallic center for complexes **7a** and **7c** may be *R* as well.

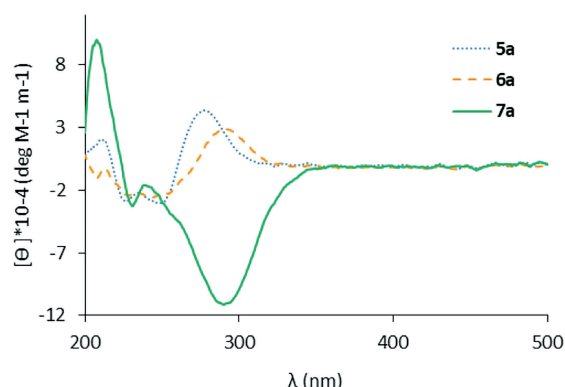


Figure 3. Circular dichroism (CD) spectra of compounds **5a**, **6a**, and **7a** (10  $\mu$ M solutions in MeCN, T = 25 $^{\circ}$  C).

The photophysical properties of compounds **5**, **6** and **7** were studied next. Figure 4 shows the absorption spectra of compounds **5**, **6** and **7**, as well as BODIPY **8**. All of them show an absorption pattern analogous to the BODIPYs,<sup>[20]</sup> with narrow absorption bands in the region of 467–498 nm composed by two maximum absorptions. The first one and most intense (496–498 nm) is attributable to the vibrational band 0–0 from the electronic transition  $S_0 \rightarrow S_1$ . The second absorption centered at 467–470 nm is assignable to the vibrational band 0–1 of the same electronic transition. It is worthy to note that the UV/Vis spectra in the 460–500 nm region of non-metallated triazoles **5** and triazolium salts **6** are analogous to the spectra of the cyclometallated compounds **7**. This fact points to a lack of conjugation between the BODIPY and the metallacycle in all derivatives. Further, complex **7c** has an absorption that is double to the equivalent absorptions in complexes **7a** and **7b**, as

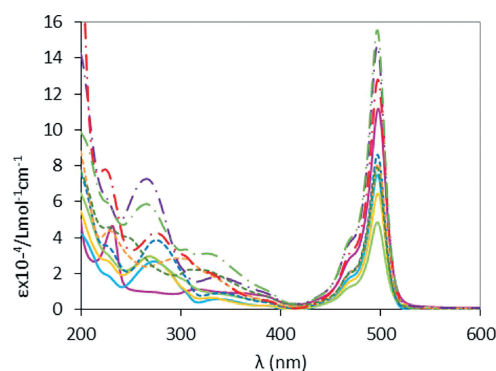


Figure 4. Absorption spectra (MeCN) of compounds **5** and **6** and complexes **7**.

expected due to the presence of two BODIPY units in its structure.

Time-dependent DFT (TD-DFT) calculations were carried out on compounds **5a–b**, **6a–b** and **7a–b** to determine the origin of the vertical transitions associated with the experimental UV/Vis absorptions. The computed transitions nicely agree with the above assignment.

Thus, the band at ca. 500 nm in compounds **5** and **6** is derived from the one electron promotion from the HOMO to the LUMO, which can be regarded as  $\pi$  and  $\pi^*$  molecular orbitals fully delocalized in the indacene moiety (see the Figure 5). Analogous orbitals are involved in the HOMO-LUMO vertical transition in the parent BODIPY **8**,<sup>[14]</sup> which is an additional proof of the exclusive involvement of the indacene moiety in the absorptions around 500 nm. It is noteworthy, that similarly to our previously reported compounds **III**, the contribution from the aryl fragment attached to the BODIPYs **5** and **6** is negligible. Additionally, the band around 500 nm in compounds **7a** and **7b** can be assigned to the HOMO-2 to LUMO and HOMO-1 to LUMO, respectively, which are also  $\pi \rightarrow \pi^*$  transitions, with both orbitals confined to the BODIPY moiety. Therefore, also in these cases, in which we have a MIC in the coordination sphere of the metal, the metal fragment is a mere spectator. These results clearly confirm that the  $\pi$ -conjugation between the metal centers and the BODIPY fragment is practically negligible. This fact has relevance in the quenching of fluorescence (see below) since a through-skeleton Dexter mechanism for the quenching may be discarded.

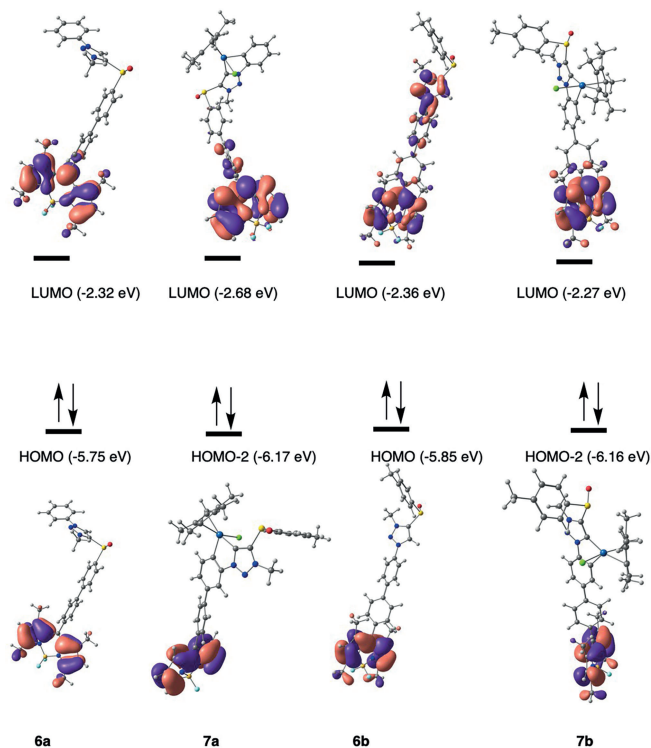


Figure 5. Orbital description of the main absorption transitions on compounds **6** and **7**.

The fluorescence of complexes **5**, **6** and **7** was measured 211 next. Figure 6 compiles the emission spectra of these complexes, together with the emission BODIPY **8** for comparison.

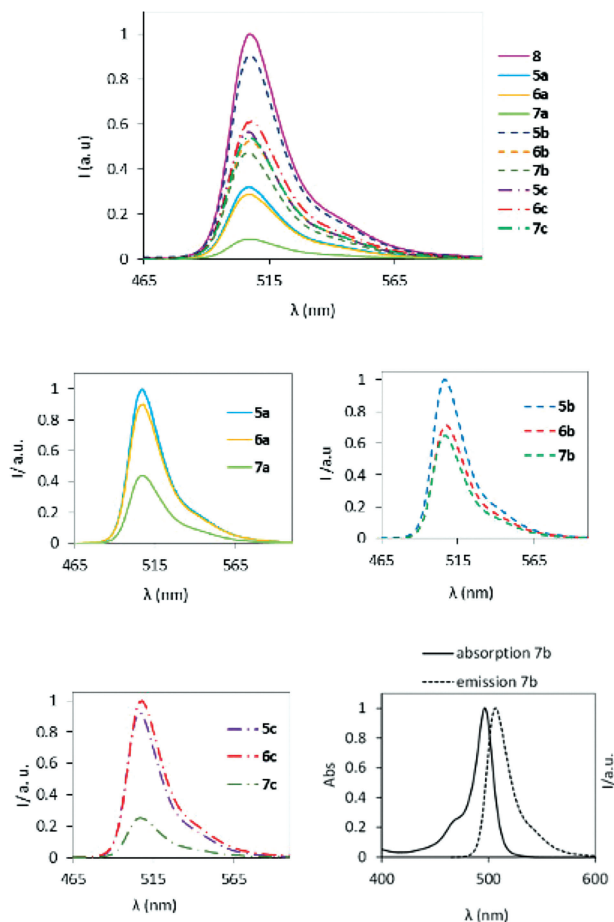


Figure 6. Emission spectra of compounds **5**, **6**, and **7**. The last graphic represents normalized absorption (—) and emission (---) spectra of compound **7b** (bottom right).

All compounds show narrow emission bands with specular symmetry respect to the absorption bands, a situation that is characteristic of the BODIPYs. The emission bands have maximums at 507–508 nm which corresponds to small Stokes shifts (9–10 nm). Again, the presence of the metal does not significantly disturb the profile of the spectra of the BODIPY, except for a slight bathochromic displacement of the triazolium salts **6** respect to triazoles **5** or Ir(III) complexes **7** (Table 1).

The emission spectra of complexes **7** show interesting properties (see Table 1). Thus, as expected due to the presence of the metal, complexes **7a** and **7c** experience a strong quenching of the fluorescence ( $f = 0.19$ ) respect the corresponding triazoles **5a**, **5c** ( $f = 0.69$  and  $f = 0.55$ , respectively) and triazolium salts **6a**, **6c** ( $f = 0.52$  and  $f = 0.51$ , respectively). In clear contrast emission of Ir(III) complex **7b** ( $f = 0.51$ ) is slightly decreased respect to that of its precursors, namely triazole **5b** and triazolium salt **6b** ( $f = 0.70$  and  $f = 0.55$ , respectively). These results show a clear dependence of the deactivation of the emission process of these complexes with the spatial structure, which may point to a Förster deactivation mechanism.<sup>[3]</sup>

Table 1. Photophysical data of compounds **5–7**.<sup>[a]</sup>

Compound	$\lambda_{\text{abs}}$ [nm] <sup>[b]</sup>	$\epsilon_{\text{abs}}$ <sup>[c]</sup>	$\lambda_{\text{em}}$ [nm] <sup>[d]</sup>	$\Phi_{\text{F}}$ <sup>[e]</sup>
<b>5a</b>	497 (429) <sup>[g]</sup>	7.48 (0.61) <sup>[f]</sup>	507	0.69
<b>6a</b>	497 (429) <sup>[g]</sup>	6.44 (0.70) <sup>[f]</sup>	508	0.52
<b>7a</b>	497 (420) <sup>[g]</sup>	4.87 (0.69) <sup>[f]</sup>	508	0.19
<b>5b</b>	497 (429) <sup>[g]</sup>	8.64 (0.70) <sup>[f]</sup>	507	0.7
<b>6b</b>	497 (431) <sup>[g]</sup>	8.13 (0.70) <sup>[f]</sup>	508	0.55
<b>7b</b>	497 (429) <sup>[g]</sup>	7.87 (0.70) <sup>[f]</sup>	507	0.51
<b>5c</b>	497	14.77	507	0.62
<b>6c</b>	497	12.79	508	0.63
<b>7c</b>	497	15.51	507	0.19

[a] All samples were measured at 25 °C in MeCN (concentration of  $10^{-5}$  M, optical density < 0.1). [b] Maximum of the UV/Vis spectrum. [c] Molar extinction coefficient  $\epsilon$  ( $\text{M}^{-1} \text{cm}^{-1} \times 10^4$ ). [d] Maximum of the emission spectrum using  $\lambda_{\text{exc}} = 450$  nm. [e] Quantum yields ( $\Phi_{\text{F}}$ ), determined using a 0.1 M solution of fluorescein in NaOH ( $\Phi_{\text{R}} = 0.95$ ) as reference. [f] Calculated TD-DFT oscillator strength. [g] Calculated TD-DFT excitation energy.

To understand the quenching mechanism, we registered the UV/Vis spectra of complex **9** (the donor in the Ir(III)-BODIPY donor-acceptor system) and the emission spectra of 4-bromo-phenyl-BODIPY **8** (the acceptor in the Ir(III)-BODIPY donor-acceptor system) (Figure 7).

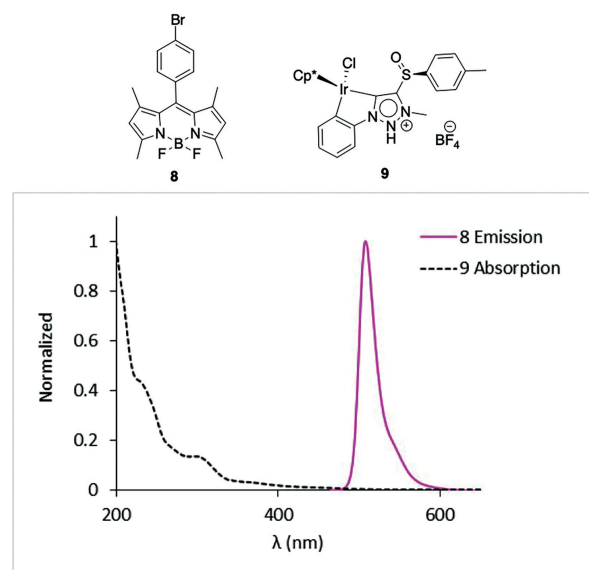


Figure 7. The absorption spectra of complex **9** and the emission spectrum of complex **8** that shows no overlapping between both spectra.

As can be seen in Figure 6, there is no significant overlapping between both absorption and emission spectra which makes the energy transfer either by a through space (Förster) or through skeleton (Dexter) improbable (see above). Therefore, the quenching of the fluorescence in complexes **7a** and **7c** is likely due to a photoinduced electron transfer mechanism (PET).

To determine the role of a PET mechanism in the fluorescence deactivation of compounds **7a** and **7c**, we computed the HOMO and LUMO of these fragments, where HOMOs of complexes **9** and **10** (compound with an additional phenyl group to determine the influence of the addition of an aromatic group on the emissive properties of the complexes). Figure 8 depicts the HOMO and LUMO of these fragments, where HOMOs of complexes **9** and **10**

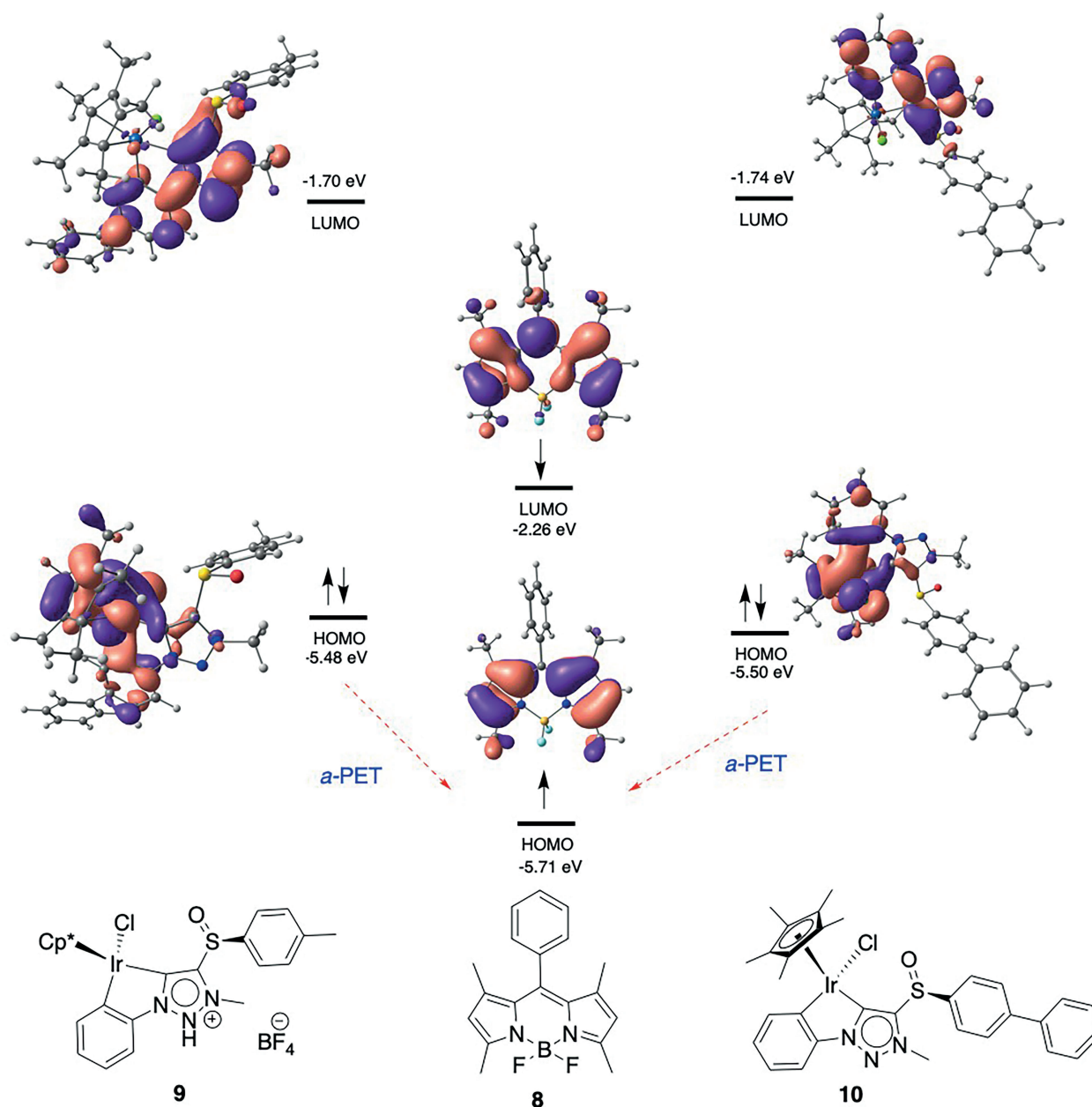


Figure 8. Orbital distribution and HOMO-LUMO energies of BODIPY **8**, complex **9**, and complex **10**.

**10** are higher in energy than the HOMO of the BODIPY **8**. As a consequence, the excitation of the BODIPY core may result in an energetically favorable IMET (intramolecular electron transfer) process from the metallacycle to the BODIPY ( $\Delta E = 0.21$  and  $0.23$  eV, respectively). Based in these results, the BODIPY fragment in complexes **7a** and **7c** may act, upon excitation, as an electron acceptor and the fluorescence may be quenched through an acceptor-excited PET (*a*-PET,  $f < 0.1$ ).

However, the extension of the PET mechanism is strongly dependent on the position of the BODIPY moiety. According to the model in Figure 8, the fluorescence of complex **7b** would be quenched by the effect of the metal atom (as in complex **7a**). Moreover, the fluorescence complex **7c**, with similar structural features to complexes **7a** and **7b** is quenched. This fact

points to the role of the moiety similar to **7a** as the fluorescence quenching element, overcoming the role of the moiety similar to **7b** in maintaining the emissive properties of the compound. To this moment, the reasons behind this strong differential behavior in closely related complexes remain elusive.

Finally, all attempts to detect CPL in complexes **7** either with 271 lineal horizontal/vertical or circular polarization, as well as with circular excitation and detection meet with no avail.

## Conclusions

The synthesis of enantiomerically pure Ir(III) complexes having one or two BODIPY moieties in their structures has been

achieved through the enantioselective C–H insertion from homochiral triazolium salts **6**. These homochiral salts are easily available through the Cu-catalyzed alkyne-azide cycloaddition (CuAAC) of an in situ generated azide (from the corresponding amine and nonaflyl azide) and alkynyl sulfoxide **1**. The BODIPY moiety was incorporated into the preformed triazol by a Suzuki coupling using BODIPY aryl boronic acid **4**. Homochiral salts **6a–c** were obtained by methylation with Me<sub>3</sub>OBF<sub>4</sub>. Homochiral salt **7c** with two BODIPY moieties was accessed by a double Suzuki coupling using boronic acid **4** which incorporated both BODIPY moieties and triazole **2c** followed by methylation.

Complexes **7a–c** were obtained as single enantiomers. The absolute configuration at the metal was established by using a combination of CD and X-ray diffraction. The optical properties of these complexes were thoroughly studied. Thus, complexes **7a** and **7c** show a significant quenching of fluorescence respect to their precursors, namely triazoles **5a** and **5c**, as well as the corresponding triazolium salts **6a** and **6c** that were strongly fluorescent. Meanwhile, the fluorescence of complex **7b** is only slightly decreased respect to the fluorescent precursors **5b** and **6b**. Based on extensive TD-DFT and DFT computations, the quenching of fluorescence in complexes **7a** and **7c** upon introduction of the Ir(III) fragment could be explained through a  $\alpha$ -PET mechanism. However, the persistence of the fluorescence in complex **7b** is still not well understood. The fluorescence of complex **7b** is striking, not only due to the close resemblance between complexes **7a** and **7b**, but due to the fact that the fluorescence of complex **7c** having the structural features of complexes **7a** (strong quenching of fluorescence) and **7b** (emissive) is quenched, like in complex **7a**. To the best of our knowledge complex **7b** is the single example of a fluorescent homochiral Ir(III) complex.<sup>[21]</sup>

Efforts to prepare other homochiral fluorescent metal-BODIPY complexes in search of CPL properties are now underway in our laboratories.

## Experimental Section

**General.** Unless noted otherwise, all manipulations were carried out under argon atmosphere using standard Schlenk techniques. CH<sub>3</sub>CN, THF and DCM were dried by passage through solvent purification columns containing activated alumina. Other solvents were HPLC grade and were used without purification. All reagents were obtained from commercial sources and used without additional purification, unless noted otherwise. Flash column chromatography was performed using silica gel (Merck, n° 9385, 230–400 mesh). <sup>1</sup>H and <sup>13</sup>C NMR spectra were recorded at 300, 400 or 500 MHz (<sup>1</sup>H NMR) and at 75, 100 or 126 MHz (<sup>13</sup>C NMR) using CDCl<sub>3</sub> and CD<sub>3</sub>CN as solvents with the residual solvent signal as internal reference (CDCl<sub>3</sub>, 7.26 and 77.2 ppm; CD<sub>3</sub>CN, 1.94 and 118.69 ppm). The following abbreviations are used to describe peak patterns when appropriate: s (singlet), d (doublet), t (triplet), q (quadruplet), m (multiplet), and br s (broad singlet). High-resolution mass spectrometry (HRMS) by the ESI technique was performed with an Agilent 6500 accurate mass apparatus with a Q-TOF analyser. IR spectra were recorded on a Perkin-Elmer 681 spectrophotometer. Optical rotations were measured on a Jasco P-2000 polarimeter using a sodium lamp. Circular Dichroism curves were obtained on a Jasco J-815 Spectropolarimeter. Melting points were determined on a

Koffler block. UV/Vis absorption spectra were registered using a UVI-CON XL spectrophotometer (Bio-Tex Instruments). Fluorescence spectra were recorded using an AMINCO Bowman Series 2 spectrofluorometer, with 1.0 nm bandwidth for emission and excitation.

Alkynes **1a** and **1b**,<sup>[22]</sup> triazole **3a**<sup>[10]</sup> and BODIPY **4**<sup>[23]</sup> were prepared according to previously described procedures.

**1,2,3-Triazole (3b).** A solution of 4-bromoaniline (0.70 g, 4.07 mmol) in H<sub>2</sub>O (8.0 mL)/MeOH (12.0 mL) was treated with 341 NaHCO<sub>3</sub> (1.37 g, 16.28 mmol), NfN<sub>3</sub> (1.99 g, 6.10 mmol) in Et<sub>2</sub>O (20.0 mL) and CuSO<sub>4</sub>·5H<sub>2</sub>O (0.10 g, 0.401 mmol). After 6 h of stirring, alkyne **1b** (0.735 g, 4.48 mmol) and sodium L-ascorbate (1.21 mg, 6.11 mmol) were added. The mixture was stirred for another 18 h. The residue was concentrated under reduced pressure, dissolved in 346 CH<sub>2</sub>Cl<sub>2</sub>, washed with a NaHCO<sub>3</sub> saturated aqueous solution, dried and concentrated under vacuum. After flash chromatography (hexanes/EtOAc/CH<sub>2</sub>Cl<sub>2</sub>, 5:2:3, v/v/v), pure triazol **3b** (0.95 g, 66 %) was obtained as a light brown solid.

<sup>1</sup>H NMR (400 MHz, CDCl<sub>3</sub>):  $\delta$  8.29 (s, 1H, N<sub>3</sub>C=CH), 7.70 (d,  $J$  = 8.0 Hz, 2H, Ar *p*-tol), 7.64 (d,  $J$  = 8.9 Hz, 2H, Ar *p*-Br-C<sub>6</sub>H<sub>4</sub>), 7.58 (d,  $J$  = 8.9 Hz, 2H, Ar *p*-Br-C<sub>6</sub>H<sub>4</sub>), 7.33 (d,  $J$  = 7.9 Hz, 2H, Ar *p*-tol), 2.40 (s, 3H, CH<sub>3</sub>, *p*-tol). <sup>13</sup>C NMR (101 MHz, CDCl<sub>3</sub>):  $\delta$  = 154.5 (C, N<sub>3</sub>C=CH), 142.5 (C, *p*-tol), 139.9 (C, *p*-tol), 135.4 (C, *p*-Br-C<sub>6</sub>H<sub>4</sub>), 133.2 (2CH, Ar *p*-Br-C<sub>6</sub>H<sub>4</sub>), 130.3 (2CH, Ar *p*-tol), 124.9 (2CH, Ar *p*-tol), 123.4 (C, *p*-Br-C<sub>6</sub>H<sub>4</sub>), 122.2 (2CH, Ar *p*-Br-C<sub>6</sub>H<sub>4</sub>), 122.0 (CH, N<sub>3</sub>C=CH), 21.6 (CH<sub>3</sub>, *p*-tol). IR (KBr):  $\nu_{\text{max}}$  1900, 1739, 1593, 1498, 1236, 1032, 819 cm<sup>-1</sup>. [ $\alpha$ ]<sub>D</sub><sup>25</sup> = +230.77 (c 0.73 CHCl<sub>3</sub>). HRMS (ESI)  $m/z$  calcd. for C<sub>15</sub>H<sub>12</sub>BrN<sub>3</sub>OS: 363.9937 [M + H]<sup>+</sup>, found 363.9946. M.p: 175–177 °C.

**BODIPY-1,2,3-triazole (5b).** A mixture of triazole **3b** (299 mg, 361 0.83 mmol) and BODIPY **4** (340 mg, 0.76 mmol) in the presence of K<sub>2</sub>CO<sub>3</sub> (418 mg, 3.02 mmol) and Pd(PPh<sub>3</sub>)<sub>4</sub> (53 mg, 0.045 mmol) in toluene (18.0 mL), EtOH (9.0 mL) and H<sub>2</sub>O (14.5 mL) was stirred at 90 °C overnight. The mixture was filtered through a pad of Celite, diluted with CH<sub>2</sub>Cl<sub>2</sub> and washed with H<sub>2</sub>O and brine. The organic 366 phase was dried with anhydrous Na<sub>2</sub>SO<sub>4</sub>, filtered and solvents removed under vacuum. After flash chromatography (hexanes/EtOAc, 3:2), pure compound **5b** (363 mg, 79 %) was obtained as a deep orange solid.

<sup>1</sup>H NMR (400 MHz, CDCl<sub>3</sub>):  $\delta$  8.33 (s, 1H, N<sub>3</sub>C=CH), 7.82 (s, 4H, Ar), 371 7.76 (m, 4H, Ar), 7.40 (d,  $J$  = 6.7 Hz, 2H, Ar *p*-tol), 7.36 (d,  $J$  = 8.2 Hz, 2H, Ar *p*-tol), 6.00 (s, 2H, BODIPY), 2.57 (s, 6H, 2CH<sub>3</sub> BODIPY), 2.42 (s, 3H, CH<sub>3</sub> *p*-tol), 1.44 (s, 6H, 2CH<sub>3</sub> BODIPY). <sup>13</sup>C NMR (101 MHz, CDCl<sub>3</sub>):  $\delta$  = 155.8 (2C, Ar BODIPY), 154.4 (C, N<sub>3</sub>C=CH), 143.1 (2C, Ar BODIPY), 142.5 (C, Ar *p*-tol), 141.4 (C, Ar), 141.0 (C, Ar), 140.0 (C, Ar), 376 139.9 (C, Ar), 136.0 (C, Ar), 135.1 (C, Ar), 131.5 (2C, Ar BODIPY), 130.4 (2CH, Ar *p*-tol), 129.0 (2CH, Ar *p*-tol), 128.6 (2CH, Ar), 127.8 (2CH, Ar), 124.9 (2CH, Ar), 121.9 (CH, N<sub>3</sub>C=CH), 121.5 (2CH, Ar BODIPY), 121.1 (2CH, Ar), 21.6 (CH<sub>3</sub>, *p*-tol), 14.7 (4CH<sub>3</sub>, BODIPY). IR (KBr):  $\nu_{\text{max}}$  1543, 1511, 1470, 1306, 1196, 1157, 982, 823, 810 cm<sup>-1</sup>. [ $\alpha$ ]<sub>D</sub><sup>25</sup> = 381 +173.88 (c 1.01, CHCl<sub>3</sub>). HRMS (ESI)  $m/z$  calcd. for C<sub>34</sub>H<sub>30</sub>BF<sub>2</sub>N<sub>5</sub>OS: 606.2311 [M + H]<sup>+</sup>, found 606.2329. M.p: Decomposes.

**BODIPY-1,2,3-triazolium salt (6b).** Triazole **5b** (202 mg, 0.33 mmol) was treated with Meerwein salt (73 mg, 0.50 mmol) in CH<sub>2</sub>Cl<sub>2</sub> (20.0 mL) at r.t. until completion of the reaction (TLC analysis). The reaction was quenched with a few drops of methanol and the solvents were removed under vacuum. The residue was solved in the minimum amount of CH<sub>2</sub>Cl<sub>2</sub> and precipitated with Et<sub>2</sub>O. Solvents were poured off and the solid washed with Et<sub>2</sub>O and dried under vacuum. After flash chromatography (MeOH/CH<sub>2</sub>Cl<sub>2</sub> 5 % v), 391 pure **6b** (85 mg, 37 %) was obtained as a reddish orange solid.

<sup>1</sup>H NMR (500 MHz, CD<sub>3</sub>CN):  $\delta$  8.90 (s, 1H, N<sub>3</sub>C=CH), 8.02 (d,  $J$  = 8.4 Hz, 2H, Ar), 7.92 (d,  $J$  = 8.5 Hz, 2H, Ar), 7.89 (d,  $J$  = 8.1 Hz, 2H,

Ar), 7.84 (d,  $J = 8.0$  Hz, 2H, Ar *p*-tol), 7.55 (d,  $J = 8.0$  Hz, 2H, Ar *p*-396 tol), 7.50 (d,  $J = 8.1$  Hz, 2H, Ar), 6.11 (s, 2H, BODIPY), 4.39 (s, 3H, N-CH<sub>3</sub>), 2.50 (s, 6H, 2CH<sub>3</sub> BODIPY), 2.48 (s, 3H, CH<sub>3</sub> *p*-tol), 1.45 (s, 6H, 2CH<sub>3</sub> BODIPY). <sup>13</sup>C NMR (126 MHz, CD<sub>3</sub>CN):  $\delta = 156.6$  (2C, Ar BODIPY), 148.2 (C, N<sub>3</sub>C=CH), 146.1 (C, Ar *p*-tol), 144.8 (C, Ar), 144.5 (2C, Ar BODIPY), 142.6 (C, Ar), 140.2 (C, Ar), 136.9 (C, Ar *p*-tol), 136.1 401 (C, Ar), 135.0 (C, Ar), 132.1 (2C, Ar BODIPY), 132.0 (2CH, Ar *p*-tol), 130.1 (CH, N<sub>3</sub>C=CH), 130.0 (2CH, Ar), 129.9 (2CH, Ar), 129.0 (2CH, Ar), 126.9 (2CH, Ar *p*-tol), 123.4 (2CH, Ar), 122.4 (2CH, Ar BODIPY), 40.8 (CH<sub>3</sub>, N-CH<sub>3</sub>), 21.7 (CH<sub>3</sub>, *p*-tol), 14.8 (2CH<sub>3</sub>, BODIPY), 14.7 (2CH<sub>3</sub>, BODIPY). IR (KBr):  $\nu_{\text{max}}$  1544, 1511, 1307, 1197, 1158, 1085, 1061, 406 983, 824 cm<sup>-1</sup>.  $[\alpha]_{\text{D}}^{25} = +114.37$  (c 0.08, CHCl<sub>3</sub>). HRMS (ESI) *m/z* *calcd.* for C<sub>35</sub>H<sub>33</sub>BF<sub>2</sub>N<sub>5</sub>OS: 620.2468 [M - BF<sub>4</sub>]<sup>+</sup>, found 620.2469. M.p.: Decomposes.

**BODIPY-Iridacycle (7a).** To a solution of triazolium salt **6a** (60 mg, 0.09 mmol) in CH<sub>2</sub>Cl<sub>2</sub> (8.0 mL), [IrCl<sub>2</sub>Cp\*]<sub>2</sub> (65 mg, 0.08 mmol) and 411 Cs<sub>2</sub>CO<sub>3</sub> (68 mg, 0.21 mmol) were added. The reaction mixture was stirred at r.t. until completion of the reaction (<sup>1</sup>H NMR analysis). The mixture was filtered through a pad of Celite. Addition of NaOAc (19 mg, 0.23 mmol) and stirring for another 24 h yielded, after flash chromatography (MeOH/CH<sub>2</sub>Cl<sub>2</sub> 3 % v) pure **7a** (87 mg, 80 %) as a 416 deep orange solid.

<sup>1</sup>H NMR (400 MHz, CDCl<sub>3</sub>):  $\delta$  8.09 (d,  $J = 8.3$  Hz, 2H, Ar), 7.92 (d,  $J = 6.4$  Hz, 1H, Ar), 7.81 (d,  $J = 8.5$  Hz, 2H, Ar), 7.70 (d,  $J = 8.0$  Hz, 2H, Ar), 7.60 (dd,  $J = 7.8, 1.4$  Hz, 1H, Ar), 7.37 (d,  $J = 7.9$  Hz, 2H, Ar), 7.18 (td,  $J = 7.4, 1.4$  Hz, 1H, Ar), 7.03 (td,  $J = 7.5, 1.3$  Hz, 1H, Ar), 5.98 (s, 421 2H, BODIPY), 4.06 (s, 3H, N-CH<sub>3</sub>), 2.56 (s, 6H, 2CH<sub>3</sub> BODIPY), 1.91 (s, 15H, 5CH<sub>3</sub> Cp\*), 1.41 (s, 6H, 2CH<sub>3</sub> BODIPY). <sup>13</sup>C NMR (101 MHz, CDCl<sub>3</sub>):  $\delta = 156.2$  (C, N<sub>3</sub>C=Clr), 155.8 (2C, Ar BODIPY), 144.6 (C, Ar), 144.0 (C, Ar), 143.5 (C, N<sub>3</sub>C=Clr), 143.1 (3C, C Ar, 2C Ar BODIPY), 141.1 (C, Ar), 140.3 (C, Ar), 139.8 (C, Ar), 136.9 (CH, Ar), 135.1 (C, Ar), 426 131.5 (2C, Ar BODIPY), 129.6 (CH, Ar), 129.0 (2CH, Ar), 128.6 (2CH, Ar), 127.9 (2CH, Ar), 126.1 (2CH, Ar), 122.7 (CH, Ar), 121.5 (2CH, Ar BODIPY), 114.3 (CH, Ar), 91.6 (5C, Cp\*), 38.2 (CH<sub>3</sub>, N-CH<sub>3</sub>), 14.8 (2CH<sub>3</sub>, BODIPY), 14.7 (2CH<sub>3</sub>, BODIPY), 9.9 (5C, CH<sub>3</sub> Cp\*). IR (KBr):  $\nu_{\text{max}}$  2917, 1544, 1511, 1470, 1410, 1307, 1195, 1157, 1085, 1051, 983, 431 823 cm<sup>-1</sup>.  $[\alpha]_{\text{D}}^{25} = -367.67$  (c 0.1, CHCl<sub>3</sub>). HRMS (ESI) *m/z* *calcd.* for C<sub>44</sub>H<sub>44</sub>BF<sub>2</sub>IrN<sub>5</sub>OS: 932.2960 [M + H]<sup>+</sup>, found 932.2968. M.p.: Decomposes.

**Computational Details.** All calculations were performed at the DFT level using the M06 functional<sup>[24]</sup> with an ultrafine integration 436 grid<sup>[25]</sup> in conjunction with the D3 dispersion correction suggested by Grimme<sup>[26]</sup> 40 as implemented in Gaussian 16.<sup>[27]</sup> S, Cl and Ir atoms were described using the scalar-relativistic Stuttgart-Dresden SDD pseudopotential<sup>[28]</sup> and its associated double- $\zeta$  basis set complemented with a set of f-polarization functions.<sup>[29]</sup> The 6-31G\*\* 441 basis set was used for the H, C, N, F and O atoms.<sup>[30]</sup> All structures of the reactants, intermediates, transition states, and products were fully optimized in dichloromethane solvent ( $\epsilon = 8.93$ ) using the SMD continuum model.<sup>[31]</sup> Calculations of absorption spectra were accomplished by using the time-dependent density functional 446 theory (TD-DFT)<sup>[32]</sup> method at the same level. All energies collected in the text are Gibbs energies in dichloromethane at 298 K.

### Crystallographic details

All data were obtained using an oil-coated shock-cooled crystal of **7b** on a Bruker-AXS APEX II diffractometer with MoK<sub>α</sub> radiation ( $\lambda = 451 0.71073$  Å) at 100(2) K. The crystal structure was solved by direct methods<sup>[33]</sup> and all non-hydrogen atoms were refined anisotropically using the least-squares method on F<sup>2</sup>.<sup>[34]</sup> The absolute configuration has been refined using the Flack parameter  $x$ .<sup>[35]</sup>

**Crystal Data of 7b:** C<sub>45</sub>H<sub>46</sub>BClF<sub>2</sub>IrN<sub>5</sub>OS, MW 981.39 g/mol, orthorhombic, P2<sub>1</sub>2<sub>1</sub>2<sub>1</sub>,  $a = 9.925(1)$  Å,  $b = 20.070(2)$  Å,  $c = 21.726(2)$  456 Å,  $V = 4327.4(4)$  Å<sup>3</sup>, 28987 reflections have been measured, 8755 independent reflections, Rint = 0.0893, 525 parameters have been refined using 20 restraints, R1 ( $I > 2\sigma$ ) = 0.0548,  $wR_2$  ( $I > 2\sigma$ ) = 0.0969, R1 (all data) = 0.0776,  $wR_2$  (all data) = 0.1032, absolute structure parameter  $x = 0.013(7)$ , largest diff. peak = 1.488 e Å<sup>-3</sup>. 461

Deposition Number 2005906 (for **7b**) contains the supplementary crystallographic data for this paper. These data are provided free of charge by the joint Cambridge Crystallographic Data Centre and Fachinformationszentrum Karlsruhe Access Structures service www.ccdc.cam.ac.uk/structures. 466

**Supporting Information** (see footnote on the first page of this article): Characterization and Experimental Procedures for compounds **5c**, **6a**, **6c**, **7b**, **7c**. Circular dichroism spectra of compounds **5-7b** and **5-7c**. Copies of NMR spectra of new compounds, crystallographic details and Cartesian Coordinates (PDF). 471

### Conflict of Interest

The authors declare no conflict of interest.

### Acknowledgments

Support for this work under grants CTQ2016-77555-C2-1-R to M. A. S., CTQ2016-77555-C2-2-R to M. C. T. and CTQ2016-81797- 476 REDC Programa Redes Consolider from the AEI (Spain) is gratefully acknowledged. M. A. S. thanks the Fundación Ramón Areces for a grant from the XVII Concurso Nacional de Ayudas a la Investigación en Ciencias de la Vida y de la Materia (CIVP18A3938). Dr. Marta García-Avello thanks the AEI for one 481 FPI predoctoral grant.

**Keywords:** Chirality · Iridium · BODIPYs · Luminescence · 7 MIC-ligands

- [1] Selected reviews: a) A. Loudet, K. Burgess, *Chem. Rev.* **2007**, *107*, 4891–4932; b) G. Ulrich, R. Ziessel, A. Harriman, *Angew. Chem. Int. Ed.* **2008**, *47*, 1184–1201; *Angew. Chem.* **2008**, *120*, 1202; c) N. Boens, V. Leen, W. Dehaen, *Chem. Soc. Rev.* **2012**, *41*, 1130–1172; d) J. Zhao, K. Xu, W. Yang, Z. Wang, F. Zhong, *Chem. Soc. Rev.* **2015**, *44*, 8904–8939.
- [2] Selected recent references on the different applications of metallo-BODIPYs: a) B. Bertrand, K. Passador, C. Goze, F. Denat, E. Bodio, M. Salmain, 491 *Coord. Chem. Rev.* **2018**, *358*, 108–124; b) G. Gupta, P. Kumari, J. Y. Ryu, J. Lee, S. M. Mobin, C. Y. Lee, *Inorg. Chem.* **2019**, *58*, 8587–8595; c) J. Zhou, Y. Zhang, G. Yu, M. R. Crawley, C. R. P. Fulong, A. E. Friedman, S. Sengupta, J. Sun, Q. Li, F. Huang, T. R. Cook, *J. Am. Chem. Soc.* **2018**, *140*, 7730–7736; d) M. Zhang, S. Li, X. Yan, Z. Zhou, M. L. Saha, Y.-C. Wang, 496 P. J. Stang, *J. Am. Chem. Soc.* **2017**, *139*, 5067–5074; e) C. Y. Lee, O. K. Farha, B. J. Hong, A. A. Sarjeant, S. T. Nguyen, J. T. Hupp, *J. Am. Chem. Soc.* **2011**, *133*, 15858–15861; f) Y. Jeong, J. Yoon, *Inorg. Chim. Acta* **2012**, *381*, 2–14; g) D. Wang, R. Malmberg, I. Pernik, S. K. K. Prasad, M. Roemer, K. Venkatesan, T. W. Schmidt, S. T. Keaveney, B. A. Messerle, *Chem. Sci.* **2020**, *11*, 6256–6267; h) M. A. Filatov, *Org. Biomol. Chem.* **2020**, *18*, 10–27; i) V. N. Nemykin, T. S. Blesener, C. J. Ziegler, *Macrocyclics* **2017**, *10*, 9–26; j) G. Ghosh, K. L. Colón, A. Fuller, T. Sainuddin, E. Bradner, J. McCain, S. M. A. Monro, H. Yin, M. W. Hetu, C. G. Cameron, S. A. McFarland, *Inorg. Chem.* **2018**, *57*, 7694–7712; k) R. P. Paitandi, V. Sharma, V. D. 506 Singh, B. K. Dwivedi, S. M. Mobin, D. S. Pandey, *Dalton Trans.* **2018**, *47*, 17500–17514.
- [3] For deactivation mechanisms see: Joseph R. Lakowicz, *Principles of Fluorescence Spectroscopy*, Springer, **2006** ■■■ (≡■■■Author: please provide the publisher of this book■■■) ■■■ . 511
- [4] P. Kos, H. Plenio, *Chem. Eur. J.* **2015**, *21*, 1088–1095.



- [5] J. Godoy, V. García-López, L. Y. Wang, S. Rondeau-Gagné, S. Link, A. A. Martí, J. M. Tour, *Tetrahedron* **2015**, *71*, 5965–5972.
- [6] P. Kos, H. Plenio, *Angew. Chem. Int. Ed.* **2015**, *54*, 13293–13296; *Angew. Chem.* **2015**, *127*, 13491.
- [7] M. Navarro, S. Wang, H. Müller-Bunz, G. Redmond, P. Farràs, M. Albrecht, *Organometallics* **2017**, *36*, 1469–1478.
- [8] M. A. Sierra, M. C. De La Torre, *ACS Omega* **2019**, *4*, 12983–12994.
- [9] M. Frutos, M. G. Avello, A. Viso, R. Fernández de la Pradilla, M. C. De La Torre, M. A. Sierra, H. Gornitzka, C. Hemmert, *Org. Lett.* **2016**, *18*, 3570–3573.
- [10] M. G. Avello, M. Frutos, M. C. de la Torre, A. Viso, M. Velado, R. F. de la Pradilla, M. A. Sierra, H. Gornitzka, C. Hemmert, *Chem. Eur. J.* **2017**, *23*, 14523–14531.
- [11] M. G. Avello, M. C. la Torre, M. A. Sierra, H. Gornitzka, C. Hemmert, *Chem. Eur. J.* **2019**, *25*, 13344–13353.
- [12] G. M. Chu, A. Guerrero-Martinez, I. Fernandez, M. A. Sierra, *Chem. Eur. J.* **2014**, *20*, 1367–1375.
- [13] G. M. Chu, A. Guerrero-Martinez, C. R. De Arellano, I. Fernández, M. A. Sierra, *Inorg. Chem.* **2016**, *55*, 2737–2747.
- [14] G. M. Chu, I. Fernández, A. Guerrero-Martínez, C. Ramírez De Arellano, M. A. Sierra, *Eur. J. Inorg. Chem.* **2016**, *2016*, 844–852.
- [15] Recent reviews: a) J.-L. Ma, Q. Peng, C.-H. Zhao, *Chem. Eur. J.* **2019**, *25*, 15441–15454; b) H. Tanaka, Y. Inoue, T. Mori, *ChemPhotoChem* **2018**, *2*, 386–402.
- [16] Selected reviews: a) F. Zinna, L. Di Bari, *Chirality* **2015**, *27*, 1–13; b) R. Carr, N. H. Evans, D. Parker, *Chem. Soc. Rev.* **2012**, *41*, 7673–7686; c) Y. Kitagawa, M. Tsurui, Y. Hasegawa, *ACS Omega* **2020**, *5*, 3786–3791.
- [17] J. R. Suárez, B. Trastoy, M. E. Pérez-Ojeda, R. Marín-Barrios, J. L. Chiara, *Adv. Synth. Catal.* **2010**, *352*, 2515–2520.
- [18] J. Zhai, T. Pan, J. Zhu, Y. Xu, J. Chen, Y. Xie, Y. Qin, *Anal. Chem.* **2012**, *84*, 10214–10220.
- [19] Compounds **7** were configurationally stable in solution as determined by <sup>1</sup>H-NMR.
- [20] a) H. Lu, J. MacK, Y. Yang, Z. Shen, *Chem. Soc. Rev.* **2014**, *43*, 4778–4823; b) W. Qin, M. Baruah, A. Stefan, M. Van Der Auweraer, N. Boens, *ChemPhysChem* **2005**, *6*, 2343–2351; c) M. Kollmannsberger, K. Rurack, U. Resch-Genger, J. Daub, *J. Phys. Chem. A* **1998**, *102*, 10211–10220.
- [21] It can be thought that complexes **6** have a participation of Dexter and Förster mechanisms, which are important in complexes **6a** and **6c** and less important for complex **6b**. However, additional data to support this hypothesis will be required.
- [22] H. Kosugi, M. Kitaoka, K. Tagami, A. Takahashi, H. Uda, *J. Org. Chem.* **1987**, *52*, 1078–1082.
- [23] See ref.<sup>[18]</sup> ((=<=■Author: here was a duplicate with ref. [18]■)). 556
- [24] a) Y. Zhao, D. G. Truhlar, *Theor. Chem. Acc.* **2008**, *120*, 215–241; b) Y. Zhao, D. G. Truhlar, *Acc. Chem. Res.* **2008**, *41*, 157–167; c) Y. Zhao, D. G. Truhlar, *Chem. Phys. Lett.* **2011**, *502*, 1–13.
- [25] S. E. Wheeler, K. N. Houk, *J. Chem. Theory Comput.* **2010**, *6*, 395–404.
- [26] S. Grimme, J. Antony, S. Ehrlich, H. A. Krieg, *J. Chem. Phys.* **2010**, *132*, 561 154104.
- [27] M. J. Frisch, G. W. Trucks, H. B. Schlegel, G. E. Scuseria, M. A. Robb, J. R. Cheeseman, G. Scalmani, V. Barone, B. Mennucci, G. A. Petersson, H. Nakatsuji, M. Caricato, X. Li, H. P. Hratchian, A. F. Izmaylov, J. Bloino, G. Zheng, J. L. Sonnenberg, M. Hada, M. Ehara, K. Toyota, R. Fukuda, J. Hasegawa, M. Ishida, T. Nakajima, Y. Honda, O. Kitao, H. Nakai, T. Vreven, J. A. Montgomery Jr., J. E. Peralta, F. Ogliaro, M. Bearpark, J. J. Heyd, E. Brothers, K. N. Kudin, V. N. Staroverov, R. Kobayashi, J. Normand, K. Raghavachari, A. Rendell, J. C. Burant, S. S. Iyengar, J. Tomasi, M. Cossi, N. Rega, J. M. Millam, M. Klene, J. E. Knox, J. B. Cross, V. Bakken, C. Adamo, J. Jaramillo, R. Gomperts, R. E. Stratmann, O. Yazyev, A. J. Austin, R. Cammi, C. Pomelli, J. W. Ochterski, R. L. Martin, K. Morokuma, V. G. Zakrzewski, G. A. Voth, P. Salvador, J. J. Dannenberg, S. Dapprich, A. D. Daniels, Ö. Farkas, J. B. Foresman, J. V. Ortiz, J. Cioslowski, D. J. Fox, *Gaussian 09, Revision C.01*. Gaussian, Inc., Wallingford CT, **2016**. 576
- [28] D. Andrae, U. Häußermann, M. Dolg, H. Stoll, H. Preuß, *Theor. Chim. Acta* **1990**, *77*, 123–141.
- [29] A. W. Ehlers, M. Böhme, S. Dapprich, A. Gobbi, A. Höllwarth, V. Jonas, K. F. Köhler, R. Stegmann, A. Veldkamp, G. Frenking, *Chem. Phys. Lett.* **1993**, *208*, 111–114. 581
- [30] a) W. J. Hehre, R. Ditchfield, J. A. Pople, *J. Chem. Phys.* **1972**, *56*, 2257; b) M. M. Francl, W. J. Pietro, W. J. Hehre, J. S. Binkley, M. S. Gordon, D. J. DeFrees, J. A. Pople, *Chem. Phys.* **1982**, *77*, 3654–3665.
- [31] A. V. Marenich, C. J. Cramer, D. G. Truhlar, *J. Phys. Chem. B* **2009**, *113*, 6378–6396. 586
- [32] a) M. E. Casida, *Recent Developments and Applications of Modern Density Functional Theory*, Vol. 4, Elsevier, Amsterdam, **1996**; b) M. E. Casida, D. P. Chong, *Recent Advances in Density Functional Methods*, Vol. 1, World Scientific, Singapore, **1995**, p. 155.
- [33] G. M. Sheldrick, *Acta Crystallogr., Sect. A* **2008**, *64*, 112–122. 591
- [34] G. M. Sheldrick, *Acta Crystallogr., Sect. C* **2015**, *71*, 3–8.
- [35] S. Parsons, H. D. Flack, T. Wagner, *Acta Crystallogr., Sect. B* **2013**, *69*, 249–259.

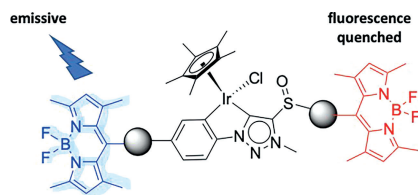
Received: August 5, 2020

596 **Luminescent Metallo-BODIPYs**

M. G. Avello, M. C. de la Torre,\*  
A. Guerrero-Martínez, M. A. Sierra,\*

601 H. Gornitzka, C. Hemmert ..... 1–10

**Chiral-at-Metal BODIPY-Based Iridium(III) Complexes: Synthesis and Luminescence Properties**



Chiral at metal, enantiomerically pure Ir(III) complexes having one or two BODIPY moieties have been prepared for the first time, using an enantioselective C–H activation reaction. Their emissive properties depend on the position of the BODIPY moiety. Fluorescence is quenched when BODIPY is attached to the substituent in the sulfoxide and maintained if attached to the substituent in the triazole ring.

611



The fluorescence of Ir BODIPY complexes prepared by de la Torre, Sierra, and co-workers depends on the attachment point of the BODIPY ligand @biorganomet

616 Share your work on social media! *The European Journal of Inorganic Chemistry* has added Twitter as a means to promote your article. Twitter is an online microblogging service that enables its users to send and read text-based messages of up to 140 characters, known as “tweets”. Please check the pre-written tweet in the galley proofs for accuracy. Should you or your institute have a Twitter account, please let us know the appropriate username (i.e., @accountname), and we will do our best to include this information in the tweet. This tweet will be posted to the journal’s Twitter account @EurJIC (follow us!) upon online publication of your article, and we recommend you to repost (“retweet”) it to alert other researchers about your publication.

**Authors:** Please check that the ORCID identifiers listed below are correct. We encourage all authors to provide an ORCID identifier for each coauthor. ORCID is a registry that provides researchers with a unique digital identifier. Some funding agencies recommend or even require the inclusion of ORCID IDs in all published articles, and authors should consult their funding agency guidelines for details. Registration is easy and free; for further information, see <http://orcid.org/>.

Marta G. Avello  
María C. de la Torre\*  
Andrés Guerrero-Martínez  
Miguel A. Sierra\* <http://orcid.org/0000-0002-3360-7795>

631 Heinz Gornitzka  
Catherine Hemmert

doi.org/10.1002/ejic.202000745